

Characteristics of amyloid-related oligomers revealed by crystal structures of macrocyclic β -sheet mimics

Cong Liu^{1,3}, Michael R. Sawaya^{1,3}, Pin-Nan Cheng², Jing Zheng², James S. Nowick², David Eisenberg^{1}*

¹ UCLA-DOE Institute for Genomics and Proteomics, Howard Hughes Medical Institute, Molecular Biology Institute, University of California, Los Angeles, Los Angeles, California, CA 90095, USA

² Department of Chemistry, University of California, Irvine, Irvine, California CA 92697-2025

³ These authors contributed equally to this work.

* e-mail: david@mbi.ucla.edu

Contents

Full citation for reference 14

Figure S1-S4

Table S1-S4

References

Full citation for reference 14

Yu, L. P.; Edalji, R.; Harlan, J. E.; Holzman, T. F.; Lopez, A. P.; Labkovsky, B.; Hillen, H.; Barghorn, S.; Ebert, U.; Richardson, P. L.; Miesbauer, L.; Solomon, L.; Bartley, D.; Walter, K.; Johnson, R. W.; Hajduk, P. J.; Olejniczak, E. T. *Biochemistry* **2009**, *48*, 1870-1877.

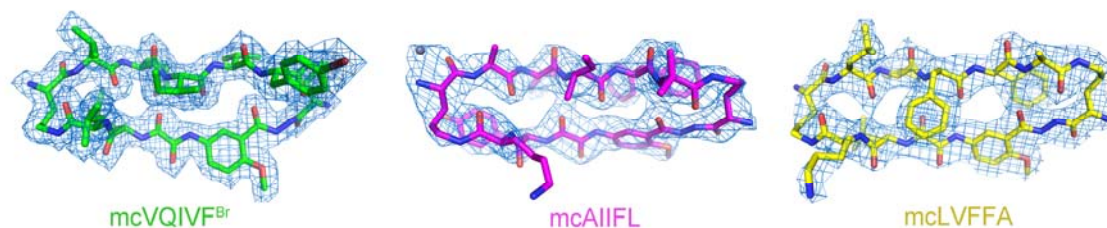


Figure S1 Electron density maps of macrocyclic peptides mcVQIVF^{Br}, mcAIIFL and mcLVFFA. The quality of each of the macrocycle models is reflected in the simulated annealing composite omit maps contoured at 1.3 σ . The resolution of the mcVQIVF^{Br} map is 2.05 Å (carbon atoms colored green), the resolution of the mcAIIFL map is 2.5 Å (carbon atoms colored magenta), and the resolution of the mcLVFFA map is 2.25 Å (carbon atoms colored yellow).

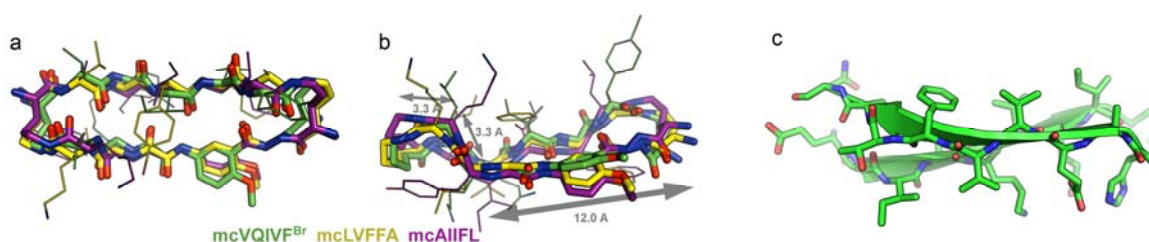


Figure S2 The superimposition of the three monomeric macrocycle structures. Stick diagram of the crystal structures of monomeric mcVQIVF^{Br}, mcLVF^{Br}FA, and mcAIIFL are shown in green, yellow and purple, respectively. (a) Side view of the superimposed structures showing the stability of the conserved framework with different insert peptides. (b) Bottom view of the superimposed structures

illustrating the bend in the blocking strand. (c) A naturally occurring β -sheet in transthyretin (PDB ID: 1BMZ) with curvature comparable to the macrocycles.

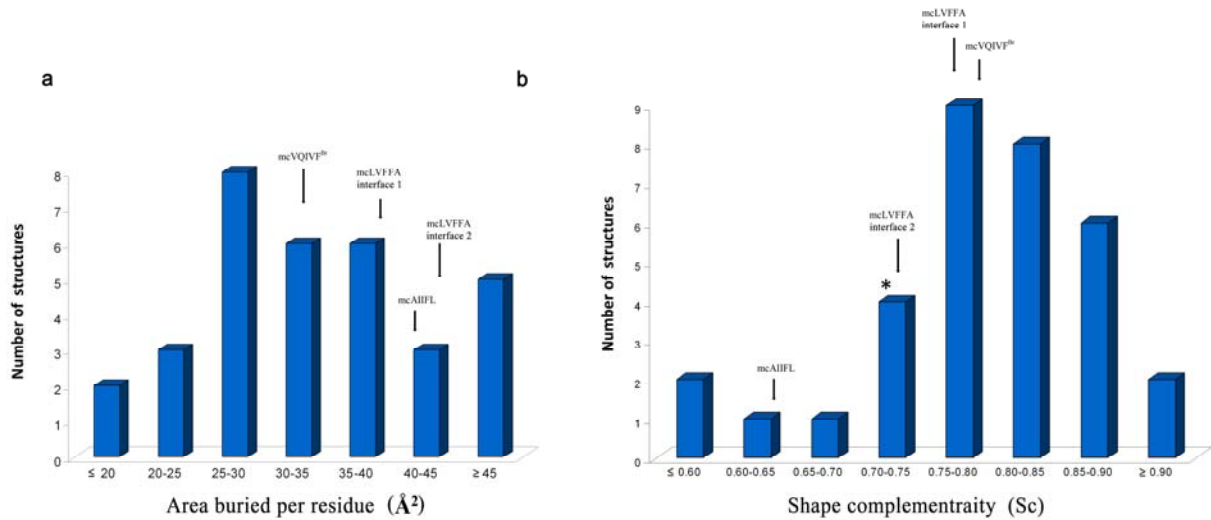


Figure S3 Comparison of area buried and shape complementarity between cross- β structures in fibrillar form and in oligomeric form. (a) 33 steric zipper structures in fibrillar form which were deposited in PDB database are chosen to draw the blue 3D-column graph¹⁻⁶. The area buried of β strand from oligomers are very similar to that from fibrils (b) 33 steric zipper structures are chosen to calculate the shape complementarity (Sc). The relatively lower Sc for mcAIFFL (0.6) might be due to relatively low resolution (2.55Å) of this structure. In other words, Sc values tend to increase slightly with improved resolution. The PDB codes of the 33 steric zipper structures are: 1YJP, 2OMM, 2OLX, 1YJO, 3HYD, 2ONX, 3FVA, 2OLX, 3DG1, 3FVA, 3FPO, 2ONW, 3HYD, 2ONV, 3NHC, 2ON9, 3DGJ, 2OL9, 3NHD, 2ONA, 2OKZ, 2OMQ, 3FQP, 3FR1, 3FTH, 2OMP, 3NVE, 3NVF, 3NVG, 3NVH, 3FTR, 3FOD, 3LOZ.

* The shape complementarities of typical oligomeric interfaces between globular proteins are between 0.70 to 0.74⁷.

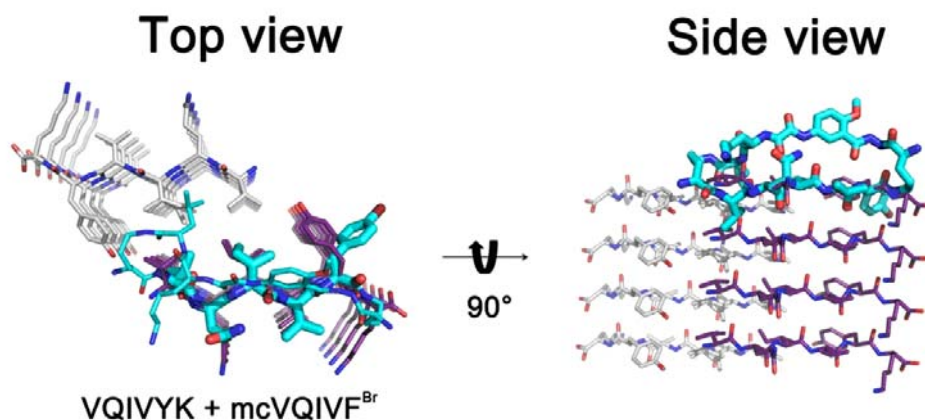


Figure S4 Overlap the amyloidogenic segment VQIVY(K) of macrocycle with steric zipper fibril structure⁴. Macrocycle is colored in cyan. For the side view (right), macrocycle is shown as stick. For the top view (left), the amyloidogenic segment of macrocycle is shown as stick and the rest part is shown as line. The steric zipper structure is shown as line. The steric zipper structure contains two layers of β -sheet. One layer is in white and the other is in purple. Each layer consists of 4 β -strands.

Table S1 Oligomeric interfaces: geometry, area buried, and shape complementarity.

Macrocycle	Symmetry class	Deviation from cross- β	Chains in interface	Sc	Area int1	Area int2	Area sum	Subtotal Hao	Subtotal Ort
mcLVFFA interface 1	5 ^a	0°	AB-to-CD	0.76	484	497	981	146	37
mcLVFFA interface 2	None ^b	15°	AB-to-EF	0.71	559	530	1089	278 ^c	2
mcVQIVF^{Br}	5 ^d	45°	A	0.77	520	520	1040	146	0
mcAIIFL	5	0°	AB-to-CD	0.60	446	448	894	12	184

^a2-fold symmetry is distorted.

^bThis interface lacks symmetry since it contains both parallel and antiparallel sheets. The parallel sheet is out of register and the identity of inward and outward-facing residues alternate between the two strands within a sheet.

^cA relatively large percentage of this interface, 41%, arises from the Hao residue, making this interface appear the least biologically relevant of the four.

^dStrands across the dry interface are orthogonal, not antiparallel.

Table S2 RMS deviations for superposed pairs of macrocycle structures.

	LVFFA	AIIFL
VQIVF ^{Br}	0.926	1.338
LVFFA	0	-
AIIFL	0.987	0

Calculation performed with LSQKAB from CCP4. The RMS deviation is calculated over the 61 pairs of atoms that are common to all three macrocycles. These include the backbone atoms of the natural amino acids and all atoms from ornithine and Hao.

Table S3 Tetrameric Interfaces: geometry, area buried, and shape complementarity.

Sequence	Symmetry class	Deviation from cross- β	Interface	Sc	Area int1	Area int2	Area sum	Subtotal Hao	Subtotal Ort
LVFFA	5 ^a	0°	AB-to-CD	0.76	484	497	981	146	37
LVFFA	None ^b	15°	AB-to-EF	0.71	559	530	1089	278	2
LVFFA	None ^b	15°	CD-to-GH	0.73	556	531	1087	301	1
LVFFA	1 ^c	45°	EF-to-GH	0.78	482	491	973	397	0
VQIVF ^{Br}	5 ^d	45°	A	0.77	520	520	1040	146	0
AIIFL	5	0°	AB-to-CD	0.60	446	448	894	12	184
AIIFL	5 ^d	45°	AB-to-EF	0.70	489	507	996	495	0

^a2-fold symmetry is distorted.

^bNone of the eight symmetry classes contain both parallel and antiparallel strands.

^cParallel strands are out of register. Furthermore, the identity of inward and outward-facing residues alternate between the two strands within a sheet. 41% of the interface arises from the Hao residue.

^dStrands across the dry interface are orthogonal, not antiparallel.

Table S4 Area buried in dry interface per strand.

Sequence	Interface	Chain	Area buried (\AA^2)
LVFFA	AB-to-CD	A:1-5	137
LVFFA	AB-to-CD	B:1-5	221
LVFFA	AB-to-CD	C:1-5	203
LVFFA	AB-to-CD	D:1-5	180
LVFFA	AB-to-CD	Average	182
LVFFA	AB-to-EF	A:1-5	211
LVFFA	AB-to-EF	B:1-5	215
LVFFA	AB-to-EF	E:1-5	192
LVFFA	AB-to-EF	F:1-5	241
LVFFA	AB-to-EF	average	215
VQIVF ^{Br}	A	A:1-5	165
AIIFL	AB-to-CD	A:1-5	214
AIIFL	AB-to-CD	B:1-5	211
AIIFL	AB-to-CD	C:1-5	217
AIIFL	AB-to-CD	D:1-5	209
AIIFL	AB-to-CD	average	213

References

1. Apostol, M.I.; Sawaya, M.R.; Cascio, D.; Eisenberg, D. *J Biol Chem* **2010**, 285, 29671-29675.
2. Ivanova, M.I.; Sievers, S.A.; Sawaya, M.R.; Wall, J.S.; Eisenberg, D. *Proc Natl Acad Sci U S A* **2009**, 106, 18990-18995.
3. Nelson, R.; Eisenberg, D. *Adv Protein Chem* **2006**, 73, 235-282.
4. Sawaya, M.R.; Sambashivan, S.; Nelson, R.; Ivanova, M.I.; Sievers, S.A.; Apostol, M.I.; Thompson, M.J.; Balbirnie, M.; Wiltzius, J.J.; McFarlane, H.T.; Madsen, A.; Riek, C.; Eisenberg, D. *Nature* **2007**, 447, 453-457.

5. Wiltzius, J.J.; Landau, M.; Nelson, R.; Sawaya, M.R.; Apostol, M.I.; Goldschmidt, L.; Soriaga, A.B.; Cascio, D.; Rajashankar, K.; Eisenberg, D. *Nat Struct Mol Biol* **2009**, 16, 973-978.
6. Wiltzius, J.J.; Sievers, S.A.; Sawaya, M.R.; Cascio, D.; Popov, D.; Riek, C.; Eisenberg, D. *Protein Sci* **2008**, 17, 1467-1474.
7. Lawrence, M.C.; Colman, P.M. *J Mol Biol* **1993**, 234, 946-950.